

Dynamic behaviour of dry sand in simple shear loading at a wide range of normal stresses

Mahmud Al Tarhouni, Bipul Hawlader, Anup Fouzder & Ashutosh Dhar
Department of Civil Engineering, Memorial University, St. John's, Newfoundland and Labrador, Canada



ABSTRACT

Dynamic properties of sand have a significant effect on many geotechnical problems. In the present study, an experimental investigation is carried out to evaluate the dynamic properties of dry sand. A series of cyclic shear tests under a constant normal stress was conducted in simple shear condition for a wide range of normal stresses (12.5 kPa–400 kPa). Multi-stage cyclic shear strain amplitudes, ranging from a low to a high value (0.005%–8%), were adopted. The results show that the shear modulus decreases with an increase in cyclic shear strain amplitude; however, an opposite trend is found for the damping ratio. The effects of normal stress and cyclic strain history on the dynamic properties of sand are discussed.

RÉSUMÉ

Les propriétés dynamiques du sable ont un effet significatif sur de nombreux problèmes géotechniques. Dans la présente étude, une investigation expérimentale est réalisée pour évaluer les propriétés dynamiques du sable sec. Une série d'essais de cisaillement cyclique sous contrainte normale constante a été réalisée dans des conditions de cisaillement simple pour une large gamme de contraintes normales (12.5 kPa à 400 kPa). Des amplitudes de déformation de cisaillement cyclique à plusieurs étages, allant de faibles à élevées (0.005% à 8%), ont été adoptées. Les résultats montrent que le module de cisaillement diminue avec une augmentation de l'amplitude de la contrainte de cisaillement cyclique; cependant, on constate une tendance opposée pour le rapport d'amortissement. Les effets de la contrainte normale et de l'historique des contraintes cycliques sur les propriétés dynamiques du sable sont discutés.

1 INTRODUCTION

Understanding the dynamic behaviour of soil is important in the geotechnical design for cyclic loading. The shear modulus and damping ratio are the commonly used parameters for modeling the cyclic behaviour of soil. The dynamic properties are highly influenced by the type of loading, drainage conditions, and soil type. Previous studies show that a number of factors such as void ratio, degree of saturation, stress level, stress and strain amplitudes, and the number of loading cycles have a significant effect on cyclic behaviour of sand. The cyclic stress–strain behaviour of sand in drained or dry conditions has been studied less as compared to the undrained cyclic response. This is mainly due to the focus on the liquefaction phenomenon of sand that could cause catastrophic failures during an earthquake (Seed and Idriss 1971; Vaid and Chern 1985; Ishihara 1993).

When a dry sand sample is subjected to cyclic loading, a decrease in volume occurs depending upon the applied cyclic shear strain amplitude (γ_a). For a moderate to large γ_a , each loading cycle might involve the nonlinear stress–strain behaviour, which could cause cyclic settlement of the soil layer in the field. Observing such settlement due to earthquake loading, studies have been performed to understand the favourable soil conditions and mechanisms behind the settlement (Silver and Seed 1971; Hsu and Vucetic 2004). Experimental studies show that volumetric compaction might occur in loose to dense sand (Silver and Seed 1971). Moreover, there is a threshold shear strain amplitude (γ_{tv}) below which volumetric compaction is negligible.

The cyclic stress–strain behaviour of sand can be studied using cyclic direct simple shear (DSS), triaxial, and hollow cylinder tests. The DSS test allows the rotation of the principal stress direction (α), similar to that occurring in the field. In previous studies, dry sand behaviour was investigated by conducting DSS tests under a constant normal stress (Sliver and Seed 1971; Seed and Silver 1972; Tokimatsu and Seed 1987; Vucetic 1994; Vucetic et al. 1998, Hsu and Vucetic 2004). The drained cyclic behaviour of fully or partially saturated soil was also investigated in some studies using the DSS apparatus (Hsu and Vucetic 2004; Kang et al. 2016). Furthermore, cyclic hollow cylinder torsional shear tests were carried out in drained condition to understand the complex behaviour of sand (Hardin and Drnevich 1972; Tatsuoka et al. 1978; Uthayakumar 1992; Teachavorasinskun et al. 1991).

Most of the data available in the literature for estimation of the dynamic properties are based on experiential investigations under medium- and high-stress levels. However, the response of many structures, for example buried pipelines is governed by the cyclic stress–strain behaviour of sand at a low-stress level. Most of the existing research and the current design guidelines do not consider the cyclic soil behaviour at low stresses; rather, the behaviour obtained for a relatively high-stress level is commonly used. One of the main reasons for this is that the laboratory tests at a low stress are challenging. However, the tests at low-stress levels are important for understanding soil behaviour and for reliable geotechnical design at shallow depths.

This paper presents experimental results of 11 cyclic DSS tests on dry sand under a constant normal stress

varying from 12.5 kPa to 400 kPa and for shear strain amplitudes of 0.005%–8.0%.

2 STRESS AND STRAIN IN CYCLIC DSS TEST

In the direct simple shear test, the vertical stress (σ'_z) is applied and then sheared horizontally, which creates shear stress (τ_{zx}) on the top and bottom horizontal surfaces. The stress–strain response makes hysteresis loops, as shown in Fig 1. As the sample remains in a set of stacked rigid rings in the present experiments, the radial stress (σ'_r) prior to shearing can be calculated as $\sigma'_r = K_0 \sigma'_z$, where K_0 is the coefficient of earth pressure at-rest. The stress ratio is defined as τ_{zx}/σ'_z . The lateral strain increment ($d\epsilon_r$) is zero in the DSS test; therefore, the vertical strain increment ($d\epsilon_z$) represents the volumetric strain increment ($d\epsilon_v$). Further details about the state of stress and strains in a DSS test are available in previous studies (Atkinson et al. 1991; Wijewickreme et al. 2013; Al Tarhouni et al. 2017).

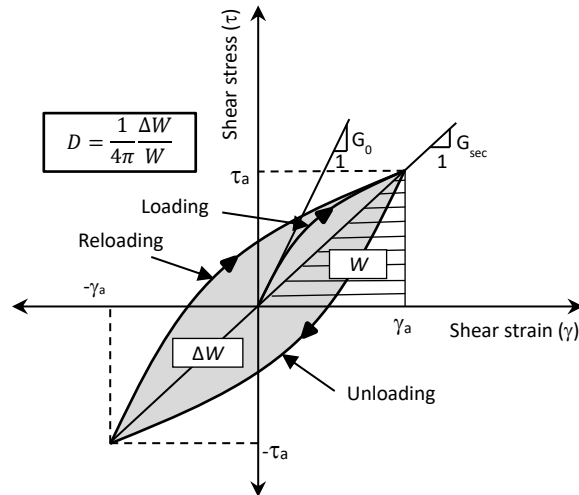


Fig. 1 Definition of shear modulus and damping ratio

The stress–strain response in cyclic simple shear tests is commonly used to compute the shear modulus and damping ratio (Fig. 1). The secant shear modulus for a given cycle (G_{sec}) is defined as the ratio of the shear stress amplitude (τ_a) to the shear strain amplitude (γ_a), which represents the average value of the shear modulus. The secant shear modulus also represents the overall inclination of the hysteresis loop and is strongly influenced by the shear strain amplitude. The damping ratio (D) represents the energy absorption in the sample (Ishihara 1996; Kramer 1996). As shown in Fig. 1, the area of the hysteresis loop (ΔW) is a measure of the energy dissipation. The maximum sorted energy (W) is considered as the area of a triangle with the base and height equal to the shear strain and shear stress amplitudes, respectively. The damping ratio is defined as $D = \frac{1}{4\pi} \frac{\Delta W}{W}$.

3 EXPERIMENTAL WORKS

3.1 Direct Simple Shear

A Combined Advanced Dynamic Cyclic Simple Shear (ADVDCSS) apparatus at Memorial University of Newfoundland is used to conduct laboratory tests. The ADVDCSS apparatus is able to conduct simple shear and triaxial tests at a low-stress level under monotonic and cyclic loading. The system has been upgraded recently by installing a dual axes 5-kN load cell to control and measure the axial and lateral loads with an accuracy better than 0.1% and resolution of 0.2 N. The ADVDCSS has a high precision feedback system for controlling stresses and displacements while maintaining a high level of accuracy. Further details of ADVDCSS apparatus specifications and capabilities have been described in Al Tarhouni et al. (2017). One of the advantages of the apparatus is that GDSLab software allows the creation of different test stages with different modules in the same test, such as the consolidation and shear stages. In this study, this feature is used to perform multi-stage cyclic shear strain amplitude tests.

3.2 Material and test procedure

A poorly graded silica sand is used in this study. The grain shape is sub-rounded to sub-angular. The mean grain size (D_{50}), uniformity coefficient (C_u), and coefficient of gradation (C_c) are 0.18 mm, 1.12, and 2.23, respectively. The specific gravity of the sand grains is 2.65. The maximum and minimum void ratios are 1.048 and 0.606, respectively, which correspond to the minimum and maximum densities of 1,294 and 1,650 kg/m³, respectively. Soil samples were prepared using a dry tamping method. The details of the sample preparation method have been described in Al Tarhouni et al. (2017). A normal stress of 3.25 kPa was applied at the initial stage to ensure proper seating of the top platen on the sample. The vertical pressure was applied gradually. The DSS tests at $\sigma'_z = 12.5, 25, 50, 100, 200, \text{ and } 400$ kPa were conducted. The relative density of the samples after consolidation (D_{rc}) was $\sim 75\%$. The cyclic shear load was applied at the bottom of the specimen, while the vertical stress was kept constant during shearing. The multi-stage shear strain amplitudes were applied with a frequency of 0.1 Hz. It is a common practice to use a frequency of 0.1 Hz for the investigation of cyclic behaviour and dynamic properties of soil under constant volume and constant stress in simple shear tests (Hsu and Vucetic 2004).

A total of 11 strain-controlled cyclic tests were conducted for varying normal stresses and shear strain amplitudes, γ_a (Table 1). The first test was conducted at $\sigma'_z = 100$ kPa and a single-stage shear strain amplitude of 1% was applied for a large number of cycles ($N = 1000$). It was found that after 100 cycles the volume change of the sample is small. A similar response has been observed in previous studies (Silver and Seed 1971; Kang et al. 2016). Therefore, in the following multi-stage tests, a maximum of 100 cycles was applied for each shear strain amplitude. The multi-stage tests were conducted under a wide range of shear strain amplitudes ($\gamma_a = 0.005\%–8\%$). The multi-

stage tests started with $\gamma_a = 0.005\%$ in T2–T4, $\gamma_a = 0.1\%$ in T5–T10 and $\gamma_a = 0.01\%$ in T11 (Table 1). In these tests, every initial shear strain amplitude can be considered as a stage with no experience of strain history. After 100 cycles in each stage, the shear strain amplitude was increased to the next higher shear strain amplitude. The purpose of applying multi-stage shear strain amplitude is to investigate the strain history effects on dynamic properties. Note that some previous studies have also investigated the effects of the strain history on dynamic properties using hollow cylinder torsional and resonant column torsional devices (Tatsuoka et al. 1979; Guzman et al. 1989; Stephenson et al. 1991; Uthayakumar 1992).

Table 1 Summary of test conditions

Test #	Normal stress (kPa)	Applied shear strain amplitude, γ_a (%)								
T1	100	-	-	-	-	-	1.0	-	-	-
T2	12.5	0.005	0.01	-	0.1	0.5	1.0	2.0	4.0	8.0
T3	25	0.005	0.01	-	0.1	0.5	1.0	2.0	4.0	8.0
T4	50	0.005	0.01	-	0.1	0.5	1.0	2.0	4.0	8.0
T5	12.5	-	-	-	0.1	0.5	1.0	2.0	4.0	8.0
T6	25	-	-	-	0.1	0.5	1.0	2.0	4.0	8.0
T7	50	-	-	-	0.1	0.5	1.0	2.0	4.0	8.0
T8	100	-	-	-	0.1	0.5	1.0	2.0	4.0	8.0
T9	200	-	-	-	0.1	0.5	1.0	2.0	4.0	8.0
T10	400	-	-	-	0.1	0.5	1.0	2.0	4.0	8.0
T11	400	-	0.01	0.05	0.1	0.5	1.0	2.0	4.0	8.0

Notes:

- i) T1 is single-stage test of 1,000 cycles
- ii) T2–T11 are multi-stage tests of 100 cycles per stage

As mentioned above, a wide range of shear strain amplitudes (0.005%–8%) was considered in this study. The goal is to investigate the dynamic response and cyclic behaviour both in small strains and nonlinear plastic zones. It should be noted that proper nonlinear modeling of dynamic response requires geotechnical properties for low to high strain levels. For example, for the liquefaction assessment, it is recommended to consider a 2.5% axial strain amplitude in triaxial tests, which is equivalent to ~3.75% shear strain amplitude (National Research Council (NRC) 1985; Ishihara 1993). The first author of this paper adopted this recommendation to investigate the cyclic behaviour of non-plastic silts in undrained simple shear loading conditions (Al Tarhouni et al., 2011). The Japanese Geotechnical Society Standards (JGS 0541-2009) suggested applying a 5% double amplitude axial shear strain in cyclic triaxial tests, which represents approximately 7.5% shear strain amplitude. Limited studies are available in the literature where the dynamic properties of sand above 1% shear strain amplitude for drained or constant normal stress conditions have been investigated by using a direct simple shear apparatus (Kang et al. 2016).

4 TEST RESULTS AND DISCUSSIONS

4.1 Typical response

4.1.1 Cyclic stress–strain behaviour

Typical stress–strain response of a dry sand specimen ($D_{rc} = 75\%$) under a constant effective stress ($\sigma'_z = 100$ kPa) for a shear strain amplitude of 1% (Test T1 in Table 1) is shown in Fig. 2. Previous studies showed that the plastic volumetric strain (densification) occurs when γ_a is greater than a threshold value of shear strain amplitude (γ_{tv}) (Hsu and Vucetic 2004). In other words, a sand specimen densifies under a moderate to large cyclic shear strain amplitude. Hsu and Vucetic (2004) showed $\gamma_{tv} \sim 0.01\% - 0.02\%$ for the different types of sands they tested.

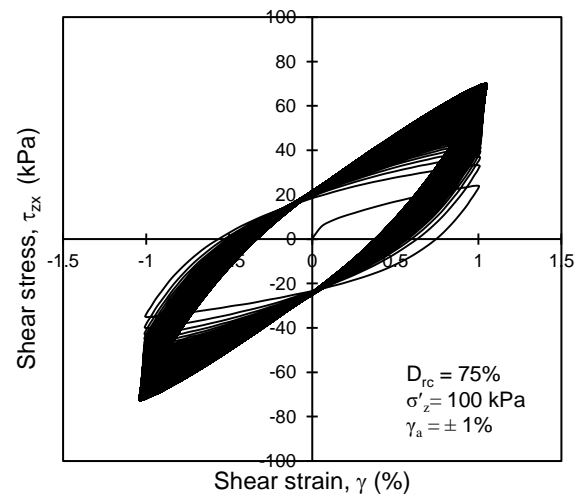


Fig. 2 Typical cyclic stress–strain response of dry sand under constant normal stress

As a considerably large $\gamma_a (= 1\%)$ is applied in this test (T1), a decrease in volume occurs in each cycle. The volume decrease occurs quickly in the first ~10 cycles; therefore, for the given shear strain amplitude the shear stress amplitude increases considerably during these cycles. In this test, a considerably large number of cycles ($N = 1,000$) were applied. However, the increase of shear stress in each cycle after ~100 cycle is small.

4.1.2 Shear Modulus variation in cyclic loading

Figure 2 shows that, in this strain-controlled test, the shear stress amplitude (τ_a) increases with the number of cycles. In other words, a sand layer in the field will be settled due to cyclic loading induced densification, which will result in an increase of shear modulus, G_{sec} (Fig. 3). For clarity, the stress–strain data for only 4 loading cycles of Fig. 2 ($N = 1, 10, 100, 1000$) are shown in Fig. 3. The shear modulus G_{sec} is ~2.5 MPa in the 1st cycle while it increases to ~6.0 MPa after 100 cycles. However, G_{sec} increases only by ~0.7 MPa in the following 900 cycles and G_{sec} is 6.7 MPa after 1000 cycles. A similar increase in shear modulus was reported from previous experimental studies (e.g., Kang et

al. 2016), which tested sands using a simple shear apparatus with radial strain measurements on the specimen. The authors also reported that G_{sec} primarily increased within the first 10 cycles in their tests.

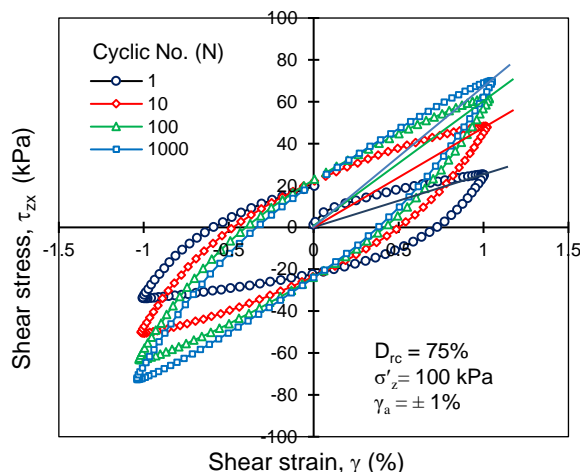


Fig. 3 Stress–strain response in single stage test T1

4.2 Effects of stress level on stress–strain behaviour

As shown in Table 1, a series of multi-stage tests (T5–T10) was performed under a normal stress of 12.5 kPa to 400 kPa. In these tests, the shear strain amplitude (γ_a) was 0.1% in the first 100 loading cycles. Figure 4 shows the stress–strain behaviour of the first cycle, which is similar to the typical response as explained in Section 4.1. The shear stress at the end of the first quarter cycle increases with an increase in normal stress. The maximum shear stress at the end of the first quarter cycle for $\sigma'_z = 400$ kPa is ~ 5.85 times of that for $\sigma'_z = 12.5$ kPa. Another observation is the difference in the shape of the stress–strain curve. For the test at a low normal stress, the slope of the stress–strain curve reduces significantly with an increase in shear strain, as compared to that at a low strain, while such a change is not observed in the test at a high normal stress. This implies that the effective stress might have a significant influence on the dynamic behaviour of soil.

4.3 Effect of normal stress and shear strain amplitude in multi-stage tests

Figure 5 shows the variation of stress ratio (τ_{zx}/σ'_z) for tests T5 and T10 which were carried out at $\sigma'_z = 12.5$ kPa and $\sigma'_z = 400$ kPa, respectively. In these tests, all other conditions, including the shear strain amplitudes and density, were the same. The hysteresis loops only for the first 15 cycles in each stage of loading are shown in this figure although 100 loading cycles were applied before moving to the next stage.

The following are the key observations. Firstly, at the low strain amplitudes (e.g., $\gamma_a = 0.1\%$), the maximum stress ratio for $\sigma'_z = 12.5$ kPa is 4.6–8.1 times that of $\sigma'_z = 400$ kPa (Fig. 5(a)). This finding agrees with the stress ratio–strain behaviour of monotonic drained loading (Al Tarhouni et al. 2017). Moreover, the stress ratio for $\sigma'_z = 12.5$ kPa

increases with the number of cycles while it remains almost constant for $\sigma'_z = 400$ kPa. Secondly, the hysteresis loop for a low γ_a is significantly larger in $\sigma'_z = 12.5$ kPa than that of $\sigma'_z = 400$ kPa. The hysteresis loops for $\sigma'_z = 400$ kPa are almost a single line; however, for $\sigma'_z = 12.5$ kPa, the stress–strain curves follow different paths for loading and unloading. Note however that the shear stress is normalized by σ'_z in Fig. 5. That is why the size of the loop is smaller in Fig. 5 for a large σ'_z . Thirdly, the shapes of the hysteresis loop for these samples are different. The shape for high-stress level is like a lens. However, for a low-stress, it is an oval shape with four segments, two almost vertical and two inclined lines. Fourthly, the size of the loop increases with an increase in shear strain amplitude (e.g., Fig. 5(f)), which implies the generation of plastic shear strain for a large γ_a . Finally, the maximum stress ratio at the end of each loading stage increases with an increase in shear strain amplitude. However, for $\sigma'_z = 12.5$ kPa, the maximum stress ratio decreases in the $\gamma_a = 4\%$ and 8% loading stages. The maximum stress ratio is almost the same (~ 0.85) for both $\sigma'_z = 12.5$ kPa and $\sigma'_z = 400$ kPa for $\gamma_a = 8\%$.

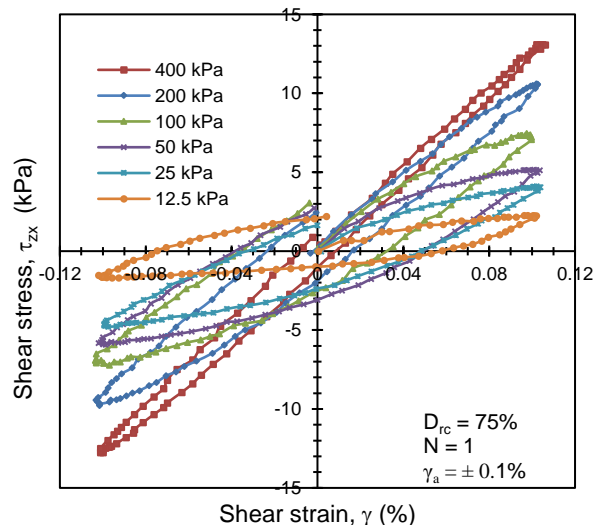


Fig. 4 Stress–strain response in the first cycle of series of multi-stage tests under a varying normal stress (T5–T10)

The discussions in Sections 4.1–4.3 suggest that the size and shape of the hysteresis loop depend on shear strain amplitude, number of cycles and normal stress, which affect the shear modulus and damping ratio that are commonly used for modeling of soil behaviour. These two parameters are further examined in the following sections based on all the results of all the tests listed in Table 1.

4.4 Effects of number of loading cycles on shear modulus

Figure 6 shows the variation of shear modulus (G_{sec}) with shear strain amplitude (γ_a) in Test T3 for four loading cycles ($N=1, 5, 10, 100$). This test was conducted at $\sigma'_z = 25$ kPa. For a given number of cycles, the shear modulus decreases with shear strain amplitude. The reduction of

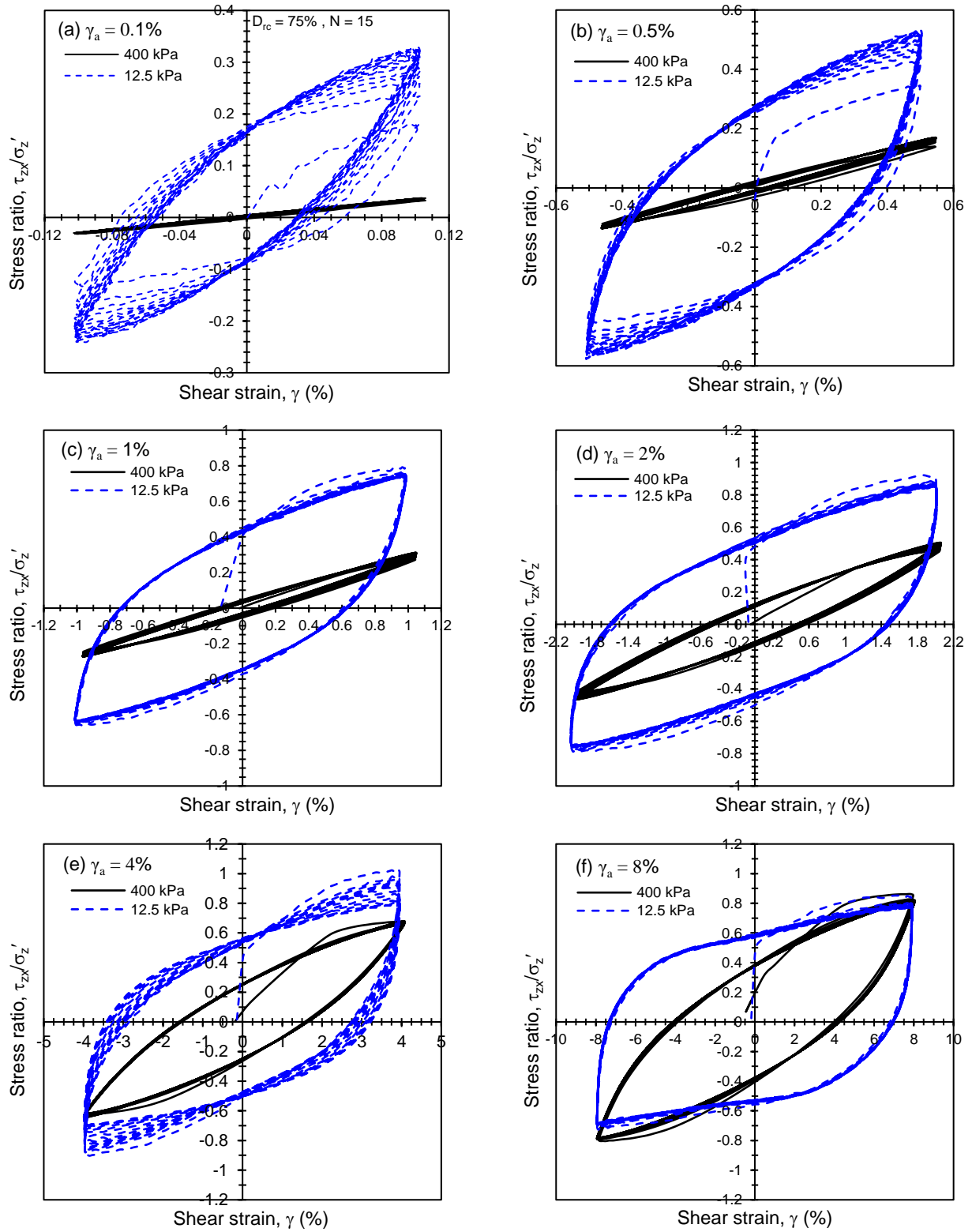


Fig. 5 Effect of stress level on stress ratio–strain behaviour

shear modulus with shear strain amplitude was also reported in previous studies based on drained simple shear tests on sand (Hardin and Drnevich 1972; Kang et al. 2016). For a given shear strain amplitude, the shear modulus increases with N . As an example, for $\gamma_a = 0.01\%$, $G_{sec} = 6.4$ MPa for $N=1$ while it is 8.77 MPa for $N = 100$. This increase is primarily due to the densification of sand with N . However, once γ_a is increased to the subsequent amplitude, G_{sec} decreases. For example, when γ_a was increased from 0.01% to 0.1%, G_{sec} reduced to 2.9 MPa for the first cycle (i.e., $N = 1$). The densification process is then continued with the loading cycle. However, for a large shear strain amplitude ($\gamma_a = 2\%$, 4% and 8%) no such increase in G_{sec} with the number of cycles was found, which is potentially due to the volume change mechanisms—both contraction and dilation occur in a single loading cycle for such a large shear strain amplitude.

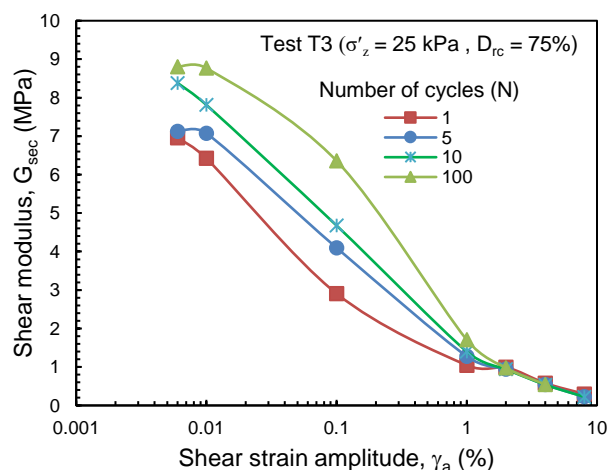


Fig. 6 Effects of shear strain amplitude and number of cycles on shear modulus

4.5 Damping ratio

As shown in Figs. 4 and 5 that the size and shape of the hysteresis loop depend on the normal stress and shear strain amplitude. The influence of these two factors is discussed in this section.

4.5.1 Effects of normal stress

The damping ratio varies with the number of cycles because of the change in size and shape of the hysteresis loop. In the present study, the damping ratio is calculated for the 15th cycle following the method described in Section 2. Figure 7 shows the variation of damping ratio for multi-stage tests (T2-T11) listed in Table 1. For at $\sigma'_z = 400$ kPa, the damping ratio is very small until $\gamma_a \sim 0.1\%$. After that, it increases rapidly, especially in the range of $\gamma_a = 1-8\%$. This can be explained from the increase in size of the hysteresis loop at a large γ_a , as shown in Fig. 5. At low-strain amplitudes, the damping ratio is significantly higher for the low normal stress cases (e.g., $\sigma'_z = 12.5$ kPa) than that of a high normal stress. Again, this is due to a large hysteresis loop in the low-stress cases (Fig. 5). Note that the dependence of damping ratio on stress level has also been

reported in previous studies (Hardin and Drnevich 1972; Kokusho 1980; Uthayakumar 1992).

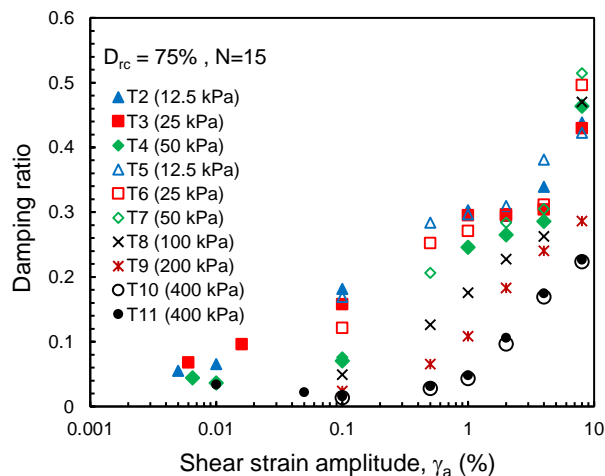


Fig. 7 Damping ratio at 15th cycle

4.5.2 Effects of strain history

As listed in Table 1, the tests T5–T7 were conducted with a first shear strain amplitude of $\gamma_{a(0)} = 0.1\%$ and then γ_a was increased in the following stages. The tests T2–T4 have similar loading stages as T5–T7; however, two additional loading stages were completed with $\gamma_a = 0.005\%$ and 0.01% prior to the stage of $\gamma_a = 0.1\%$. Therefore, these two sets of tests could be compared to investigate the effects of strain history (i.e., previous loading cycles). Similarly, T10 and T11 can be compared because T11 has two additional loading stages of $\gamma_a = 0.01\%$ and 0.05% , while T10 started with $\gamma_{a(0)} = 0.1\%$.

The solid symbols in Fig. 7 show the test results where two loading stages were completed prior to the loading stage of $\gamma_a = 0.1\%$. The open symbols represent the tests which started with $\gamma_a = 0.1\%$.

Figure 7 shows that the damping ratio is almost independent of the strain history for high normal stress cases (e.g., $\sigma'_z = 400$ kPa). However, the tests under a low normal stress show that the damping ratio is somehow influenced by the strain history (i.e., having prior additional loading cycles of lower shear strain amplitudes) although the trend is not very clear.

The effects of strain history on damping ratio is a complex process. Conducting drained cyclic torsional shear tests, Uthayakumar (1992) reported that the damping ratio is insensitive to the multi-stage loading history for the mean effective stress of 100 kPa and shear strain amplitude ranges between 0.015% and 0.2%. The present study shows that strain history has some effects on the damping ratio for low-stress level and this effect diminishes at a high-stress level.

5 CONCLUSIONS

In this paper, 10 multi-stage and one single-stage direct simple shear test results are presented. The tests were

conducted on dry sand for a wide range of normal stresses. A Combined Advanced Dynamic Cyclic Simple Shear (ADVDCSS) apparatus was used to conduct the tests. The volumetric strain primarily occurs in the first 15–20 cycles; therefore, 100 cycles were applied in each stage of the multi-stage tests. The stress ratio–strain behaviour for low normal stress is different from that of high normal stress, which also depends on shear strain amplitude. The stress ratio increases with a decrease in normal stress. The shape of the hysteresis loops also depends on normal stress, which in turn influences the damping ratio. The results show that the shear modulus decreases with an increase in cyclic shear strain amplitude; however, an opposite trend is found for the damping ratio.

6 ACKNOWLEDGMENTS

The works presented in this paper have been supported by the Natural Sciences and Engineering Research Council of Canada (NSERC), InnovateNL, the former Research and Development Corporation of Newfoundland and Labrador (RDC), the Canadian Foundation for Innovation (CFI) and the state of Libya.

7 REFERENCES

- Al Tarhouni, M., Fouzder, A., Hawlader, B., and Dhar, A. 2017. Direct simple shear and triaxial compression tests on dense silica sand at low effective stress. *GeoOttawa 70th Canadian Geotechnical Conference*, Ottawa, Canada, Oct. 1–4, 7.
- Al-Tarhouni, M., Simms, P. and Sivathayalan, S. 2011. Cyclic behaviour of reconstituted and desiccated–rewet thickened gold tailings in simple shear. *Canadian Geotechnical Journal*, 48(7): 1044–1060.
- Atkinson, J.H., Lau, W.H.W. and Powell, J.J.M. 1991. Measurement of soil strength in simple shear tests. *Canadian Geotechnical Journal*, 28(2): 255–262.
- Guzman, A.A., Chameau, J.L., Leonards, G.A. and Frost, J.D., 1989. Shear modulus and cyclic undrained behavior of sands. *Soils and Foundations*, 29(4): 105–119.
- Hardin, B.O. and Drnevich, V.P. 1972. Shear modulus and damping in soils: measurement and parameter effects. *Journal of Soil Mechanics and Foundations Div*, 98(6): 603–624.
- Hsu, C.C. and Vucetic, M., 2004. Volumetric threshold shear strain for cyclic settlement. *Journal of Geotechnical and Geoenvironmental Engineering*, 130(1):58–70.
- Ishihara, K., 1993. Liquefaction and flow failure during earthquakes. *Géotechnique*, 43(3): 351–451.
- Ishihara, K. 1996. *Soil Behaviour in Earthquake Geotechnics*, Clarendon Press, Oxford, UK
- Iwasaki, T., Tatsuoka, F., and Takagi, Y. 1978. Shear moduli of sands under cyclic torsional shear loading. *Soils and Foundations*, 18(1): 39–56.
- Japanese Geotechnical Society (JGS). 2009. Method for cyclic undrained triaxial test on soils, JGS0541-2009. Japan.
- Kang, X., Ge, L., Chang, K.T. and Kwok, A.O.L. 2016. Strain-controlled cyclic simple shear tests on sand with radial strain measurements. *Journal of Materials in Civil Engineering*, 28(4): 04015169.
- Kokusho, T. 1980. Cyclic triaxial test of dynamic soil properties for wide strain range. *Soils and Foundations*, 20(2): 45–60.
- Kramer, S.L. 1996, *Geotechnical Earthquake Engineering*. Prentice-Hall, New Jersey, USA.
- National Research Council (NRC). 1985. *Liquefaction of soils during earthquakes*. National Academy Press, Washington, D.C.
- Seed, H.B. and Idriss, I.M. 1971. Simplified procedure for evaluating soil liquefaction potential. *Journal of Soil Mechanics & Foundations*. 97(9): 1249–1273.
- Seed, H.B. and Silver, M.L., 1972. Settlement of dry sands during earthquakes. *Journal of Soil Mechanics & Foundations Div*, 98(4): 381–397.
- Silver, M.L. and Seed, H.B., 1971. Volume changes in sands during cyclic loading. *Journal of Soil Mechanics & Foundations Div.*, 97(9): 1171–1182.
- Stephenson, R.W., Stringer, S.K. and Sutterer, K., 1991. The Influence of Large Prestrains on Dynamic Properties of Sand. *Second International Conferences on Recent Advances in Geotechnical Earthquake Engineering and Soil Dynamics*. Louis, Missouri, 1921–1926.
- Tatsuoka, F., Iwasaki, T., Fukushima, S. and Sudo, H., 1979. Stress conditions and stress histories affecting shear modulus and damping of sand under cyclic loading. *Soils and Foundations*, 19(2): 29–43.
- Tatsuoka, F., Iwasaki, T. and Takagi, Y. 1978. Hysteretic damping of sands under cyclic loading and its relation to shear modulus. *Soils and Foundations*, 18(2): 25–40.
- Teachavorasinskun, S., Kato, H., Shibuya, S., Horii, N. and Tatsuoka, F. 1991. Stiffness and damping of sands in torsion shear. *International Conferences on Recent Advances in Geotechnical Earthquake Engineering and Soil Dynamics*. Louis, Missouri, 103–110.
- Tokimatsu, K. and Seed, H.B., 1987. Evaluation of settlements in sands due to earthquake shaking. *Journal of Geotechnical Engineering*, 113(8): 861–878.
- Uthayakumar, M. 1992. *Dynamic properties of sand under cyclic torsional shear*. M.Sc. Thesis. The University of British Columbia, Canada.
- Vaid, Y. P., and Chern, J.C. 1985. Cyclic and monotonic undrained response of saturated sands, *Proc. Advances in the art of testing soils under cyclic loading conditions*, ASCE, Detroit, 120–147.
- Vucetic, M. 1994. Cyclic threshold shear strains in soils. *Journal of Geotechnical Engineering*, ASCE, 120(12):2208–2228.
- Vucetic, M., Lanzo, G. and Doroudian, M. 1998. Damping at small strains in cyclic simple shear test. *Journal of Geotechnical and Geoenvironmental Engineering*, ASCE, 124(7): 585–594.
- Wijewickreme, D., Dabeet, A. and Byrne, P. 2013. Some observations on the state of stress in the direct simple shear test using 3D discrete element analysis, *Geotechnical Testing Journal*, 36(2): 292-299.